

# Implementation of superconductor-ferromagnet-superconductor $\pi$ -shifters in superconducting digital and quantum circuits

A. K. Feofanov<sup>1</sup>, V. A. Oboznov<sup>2</sup>, V. V. Bol'ginov<sup>2</sup>, J. Lisenfeld<sup>1</sup>, S.  
Poletto<sup>1</sup>, V. V. Ryazanov<sup>2</sup>, A. N. Rossolenko<sup>2</sup>, M. Khabipov<sup>3</sup>, D. Balashov<sup>3</sup>,  
A. B. Zorin<sup>3</sup>, P. N. Dmitriev<sup>4</sup>, V. P. Koshelets<sup>4</sup>, and A. V. Ustinov<sup>1</sup>

<sup>1</sup> *Physikalisches Institut and DFG Center for Functional Nanostructures (CFN),  
Karlsruhe Institute of Technology, Wolfgang-Gaede-Str.1, D-76131 Karlsruhe, Germany*

<sup>2</sup> *Institute of Solid State Physics, Russian Academy  
of Science, Chernogolovka, 142432, Russia*

<sup>3</sup> *Physikalisch-Technische Bundesanstalt,  
Bundesallee 100, 38116 Braunschweig, Germany*

<sup>4</sup> *Kotel'nikov Institute of Radio Engineering and Electronics,  
Russian Academy of Science, Mokhovaya 11,  
Building 7, Moscow, 125009, Russia*

## Abstract

The difference between the phases of superconducting order parameter plays in superconducting circuits the role similar to that played by the electrostatic potential difference required to drive a current in conventional circuits. This fundamental property can be altered by inserting in a superconducting circuit a particular type of weak link, the so-called Josephson  $\pi$ -junction having inverted current-phase relation and enabling a shift of the phase by  $\pi$ . We demonstrate the operation of three superconducting circuits – two of them are classical and one quantum – which all utilize such  $\pi$ -phase shifters realized using superconductor-ferromagnet-superconductor sandwich technology. The classical circuits are based on single-flux-quantum cells, which are shown to be scalable and compatible with conventional niobium-based superconducting electronics. The quantum circuit is a  $\pi$ -phase biased qubit, for which we observe coherent Rabi oscillations and compare the measured coherence time with that of conventional superconducting phase qubits.

The fundamental property of superconducting weak links is a  $2\pi$ -periodic current-phase relation. The supercurrent through a conventional Josephson junction is usually described by the harmonic relation  $I_s = I_c \sin \varphi$ , where  $I_c$  is the critical current. The so-called Josephson  $\pi$ -junction has the inverse current-phase relation  $I_s = I_c \sin(\varphi + \pi) = -I_c \sin \varphi$ . The  $\pi$ -junctions were theoretically proposed about three decades ago [1, 2], whereas their remarkable properties have been demonstrated in experiments notably later [3, 6, 7]. Practical implementations of  $\pi$ -junctions have been widely discussed for a variety of different technologies. These include approaches using superconductors with  $d$ -wave order parameter symmetry [3–5], circuits with nonequilibrium current injection [6], junctions with ferromagnetic tunnel barriers [7], and junctions with gated carbon nanotubes [8].

The ideas of using  $\pi$ -junctions in superconducting classical and quantum circuits have been explored in several theoretical proposals. In classical digital logic, a complementary Josephson junction inverter [9] was suggested as a superconducting analog of the complementary metal-oxide-semiconductor (CMOS) logic. It relies on using Superconducting Quantum Interference Devices (SQUIDs) of conventional (0-junctions) and  $\pi$ -types and requires having similar parameters as  $I_c$  and normal state resistance for 0- and  $\pi$ -junctions. These technologically stringent requirements can be softened by using an alternative "asymmetric" approach [10] which employs  $\pi$ -junctions as passive phase shifters (phase inverters) in basic cells of the modified Single-Flux Quantum (SFQ) logic. Here the  $\pi$ -junction critical current  $I_c$  is chosen to be much larger than that of conventional 0-junctions employed in the very same SFQ cell, so the phase difference across the  $\pi$ -junction is always close to  $\pi$  even in zero magnetic field. Since the total change of the order parameters phase over the closed path must become a multiple of  $2\pi$ , the missing phase difference of  $\pi$  or  $-\pi$  is induced on the rest part of the cell by a spontaneously generated superconducting current. A great advantage of using such  $\pi$  phase shifters is that the SFQ cell size can be significantly reduced, opening the way to scaling superconducting logic circuits down to sub- $\mu\text{m}$  dimensions [10].

The first proposal for using a loop with an integrated  $\pi$ -junction as a superconducting quantum circuit [11, 12] featured a superposition of two persistent current states in a loop at zero magnetic field, in analogy to a spin-1/2 system. The  $\pi$ -junctions required here must have very low dissipation (high normal resistance), which so far has seemed unattainable for any of the existing technologies for making  $\pi$ -junctions. The alternative usage of  $\pi$ -junctions as passive phase shifters offers an advantage for the operation of superconducting flux qubits

at the degeneracy point requiring zero or a very small external magnetic field. Potentially, this allows noise and electromagnetic interference induced by magnetic field sources to be minimized. There remains an open question: Do  $\pi$ -junctions themselves introduce any intrinsic decoherence when they are inserted into a superconduction quantum circuit?

Here we describe first practical implementation and operation of  $\pi$ -shifters in digital and quantum circuits.  $\pi$ -junctions that we use are based on superconductor-ferromagnet-superconductor (SFS) Josephson multilayer technology. The origin of the  $\pi$ -state in an SFS junction is an oscillating and sign-reversing superconducting order parameter in the ferromagnet close to the SF interface [2, 13]. Due to these oscillations, different signs of the order parameter can occur at the two banks of the SFS sandwich when the F-layer thickness is of the order of half an oscillation period, which corresponds to a sign change of the supercurrent and a negative Josephson coupling energy. This behavior was first observed experimentally on Nb-CuNi-Nb sandwiches in Ref. [7]. Further experiments reported the spontaneous flux [14] and half-periodical shifts of the superconducting interferometer  $I_c(H)$  dependence [15] as well as a sign change of the junction current-phase relation [16]. Recently, the critical current density of the Nb-Cu<sub>0.47</sub>Ni<sub>0.53</sub>-Nb  $\pi$ -junctions was pushed above 1000 A/cm<sup>2</sup> [17]. These junctions are compatible with conventional niobium thin film technology and thus can be easily integrated in the conventional fabrication process of superconducting digital circuits.

To verify the operation of  $\pi$ -junction phase shifters in an analog regime, we fabricated two geometrically identical superconducting loops on a single Si substrate (see Fig. 1(c)) schematically shown in Figs. 1(a) and (b). Circuit (b) is a two-junction interferometer conventionally called a DC-SQUID. Configuration of circuit (a) is nominally identical to (b), except that an SFS  $\pi$ -junction has been additionally inserted in the left branch of the loop seen in the lower left corner of the circuit image in Fig. 1(c). The on-chip distance between the centers of the two loops is 140  $\mu\text{m}$ , so both interferometers are exposed to the same magnetic field during the experiment. Figure 1(d) shows the schematic cross-section of a thin-film Nb-CuNi-Nb sandwich forming the  $\pi$ -junction, which fabrication procedure is described in supplementary material. The junction normal resistance  $R_n$  is about 150  $\mu\Omega$  at an F-layer thickness of 15 nm. The critical currents of such  $\pi$ -junctions are about 200  $\mu\text{A}$  and hence the junctions do not switch to the resistive state when embedded in loops with conventional tunnel junctions having critical currents of about 10  $\mu\text{A}$ . This large difference

between two critical currents means that during the dynamic switchings in the rest of the circuit,  $\pi$ -junctions do not introduce any noticeable phase shifts deviating from  $\pi$ .

The dependencies of the critical currents  $I_c(H)$  of the two devices shown in Figs. 1(a) and (b) are presented in Fig. 1(e). Whereas both curves have the same shape, they are shifted by a half-period. A small offset of the symmetry axes for both curves from the zero-field value is due to a residual magnetic field in the cryostat. The minimum of the red  $I_c(H)$  curve at zero field is due to inclusion of the  $\pi$ -junction in the superconducting loop. In the conventional SQUID the same frustrated state exists at an external magnetic field corresponding to half-integer numbers of magnetic flux quanta per cell. Thus, embedding an SFS  $\pi$  phase shifter into a superconducting loop indeed leads to self-biasing of the loop by a spontaneously induced supercurrent.

In the second experiment, we demonstrate the functionality of the  $\pi$  phase shifter included in a superconducting logic circuit. The SFQ logic circuits enable processing of information in the form of single flux quanta which can be stored in elementary superconducting cells including inductors and Josephson junctions. Dynamically, this information is represented by SFQ voltage pulses [18] having quantized area  $\int V(t)dt = \Phi_0$  and corresponding to the transfer of one flux quantum across a Josephson junction. The first SFQ circuits with active  $\pi$  elements were made of high- $T_c$  superconductor ( $\text{YBa}_2\text{Cu}_3\text{O}_{7-\delta}$ ) employing  $d$ -wave pairing symmetry combined with conventional low- $T_c$  superconductor (Nb) [19]. Operation of the circuits with the phase shifting element based on frozen flux quanta [20] has been tested earlier in Ref. [21]. Here we present the first demonstration of the functioning of an SFS  $\pi$ -phase shifter integrated in a conventional Nb SFQ circuit.

Figure 2 shows the layout and operation of our test SFQ circuit, represented by a two-stage frequency divider. The positive edges of rectangular trigger pulses ( $I_{\text{in}}$ ) are delivered to the first dividing stage of the circuit via a Josephson transmission line (left part of diagram in Fig. 2(a)) in the form of SFQ pulses. These pulses cause switching of this first stage of the circuit, the Toggle Flip-Flop (TFF) with an integrated SFS  $\pi$ -phase shifter which replaces a large inductance required in the conventional counterpart circuit for the realization of desired bistable behavior. The output signal of the first TFF in the form of SFQ pulses is sent to the second dividing stage which is realized as a conventional TFF circuit. The circuit output  $V_{\text{out}}$  time pattern shows a division of the frequency of the input pulses by four (with rather large margins for circuit parameters), which verifies its correct functioning.

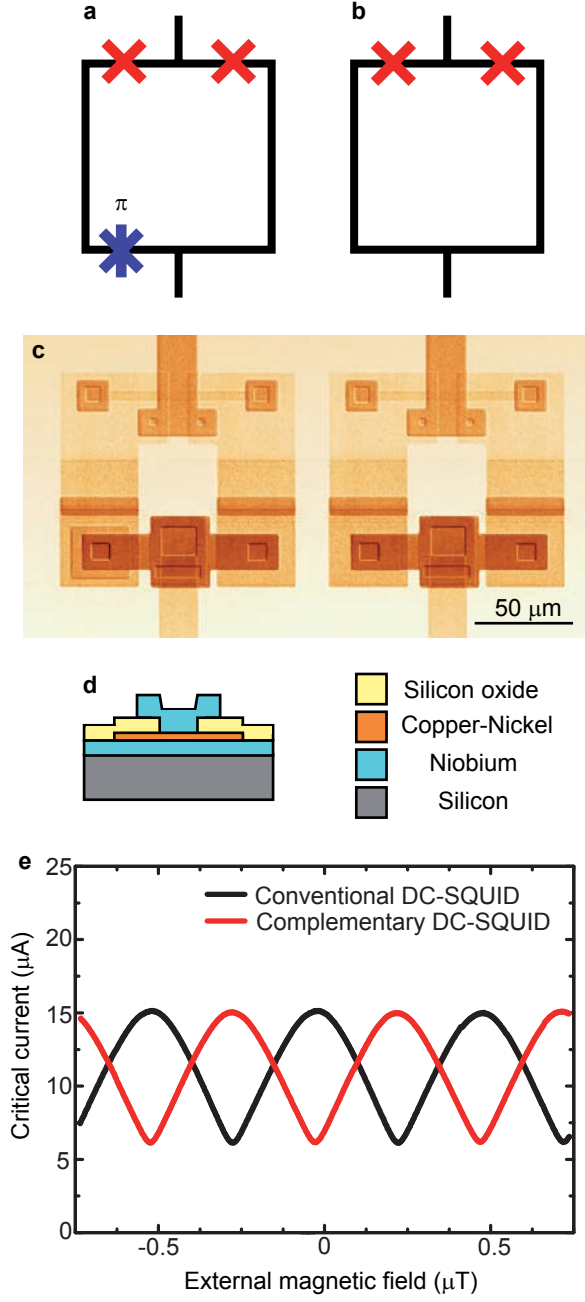


FIG. 1: Complementary DC-SQUIDs. **a**, Schematic of a complementary DC-SQUID employing two conventional Josephson junctions (red crosses) and a  $\pi$ -junction (blue star). **b**, Schematic of a conventional DC-SQUID used as a reference device. **c**, A SEM micrograph of the fabricated DC-SQUIDs. The ferromagnetic layer is visible in the lower left corner of the left device. **d**, Schematic cross-section through an SFS  $\pi$ -junction. **e**, Dependencies of the critical currents of the devices shown in **c** vs. the applied magnetic flux. The red curve related to the  $\pi$ -SQUID is shifted by half a period.

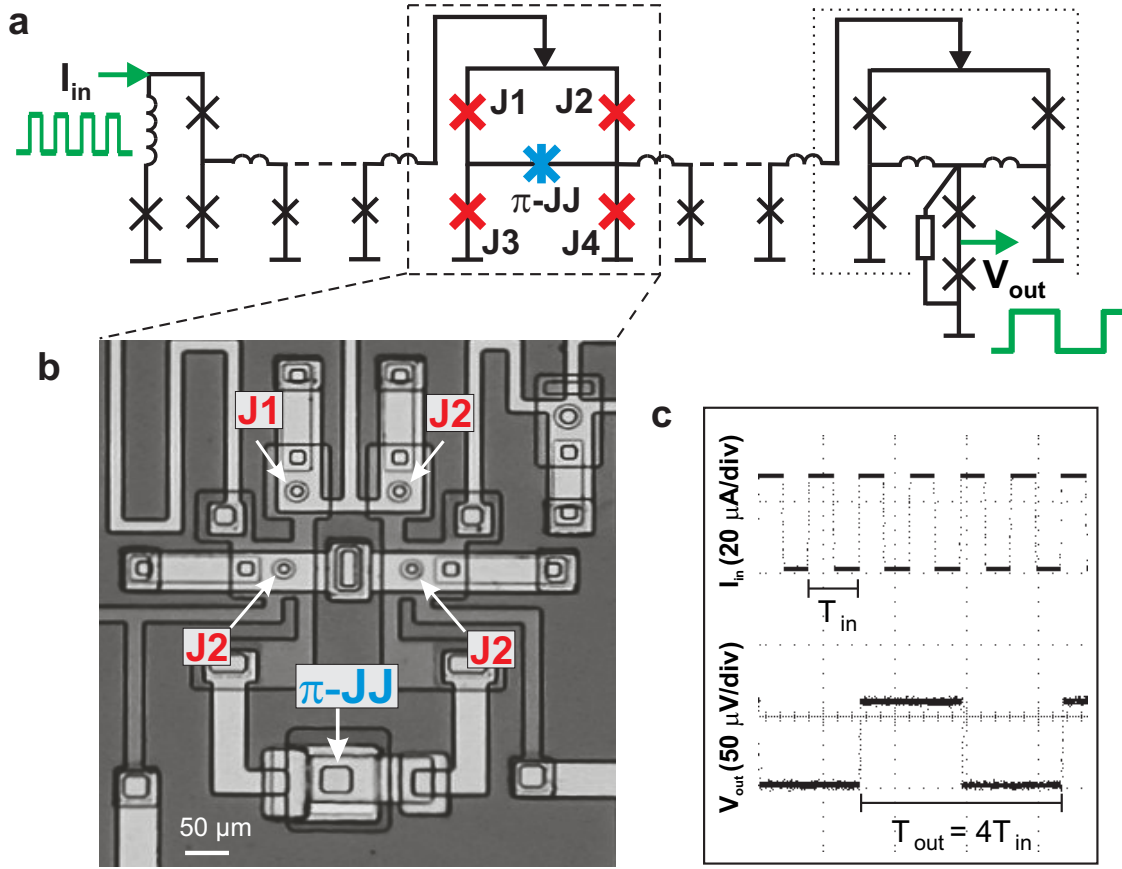


FIG. 2: **a**, Schematic of the frequency binary divider. This two-stage circuit includes the Toggle Flip-Flop (TFF) with SFS  $\pi$ -junction (inside the dash-line box) and conventional TFF (inside dotted-line box), with Josephson transmission lines enabling delivery of SFQ pulses to the inputs of TFFs. **b**, Micrograph of these TFF with  $\pi$ -junction. **c**, Oscilloscope output verifying correct operation of this SFQ circuit, i.e. division of the frequency of input pulses by four.

Another attractive application of SFS  $\pi$ -junctions is their use as phase shifters in coherent quantum circuits realizing superconducting quantum bits. The answer to the question of whether or not  $\pi$ -junctions can become useful in superconducting circuits designed for quantum computing applications depends on their impact on the coherence properties of the qubits. Potential sources of decoherence introduced by  $\pi$ -junctions can for instance be spin-flips in the ferromagnetic barrier, either occurring randomly or being driven by high-frequency currents and fields, as well as the dynamic response of the magnetic domain structure. We address these important coherence issues in a third experiment reported in

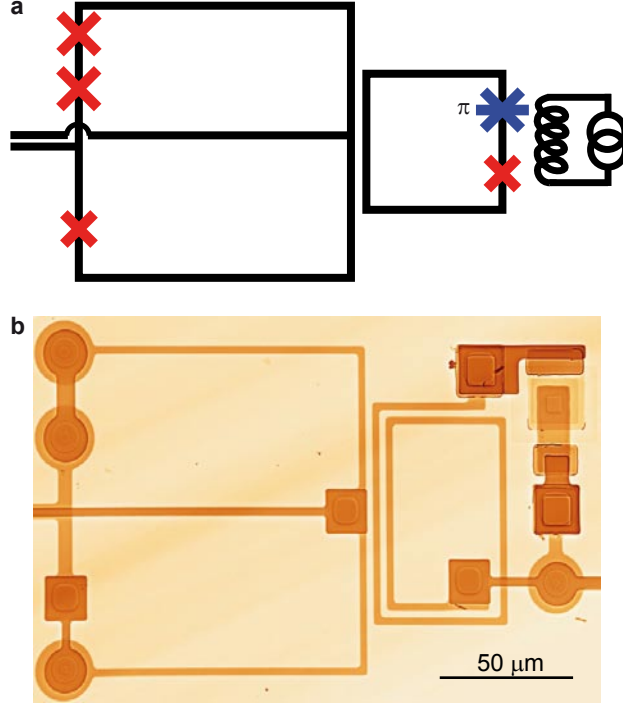


FIG. 3: Self-biased phase qubit. **a**, Schematic of a phase qubit circuit used to test the decoherence properties of the  $\pi$ -junction. The qubit is realized by the central loop with embedded conventional and  $\pi$  - Josephson junctions. The larger loop to its right is a DC-SQUID for qubit readout. A current-biased coil coupled weakly to the qubit is used for flux-biasing the qubit. **b**, SEM picture of the realized phase qubit employing a  $\pi$  - junction in the qubit loop.

this paper, in which we use an SFS  $\pi$ -junction to self-bias a superconducting phase qubit. We have chosen here a phase qubit [22] rather than a flux qubit [23] due to the simpler fabrication procedure for the former. The results reported below would nevertheless remain fully applicable to flux qubits.

A phase qubit [22] consists of a single Josephson junction embedded in a superconducting loop. It is magnetically biased close to an integer number of flux quanta in the loop. At such a bias, the potential energy of the qubit exhibits an asymmetric double-well potential, whereas two quantized energy eigenvalues of the phase localized inside only the shallow well are used as the logical qubit states  $|0\rangle$  and  $|1\rangle$ . The qubit is controlled by inducing a small-amplitude microwave current in the loop whose frequency is tuned in resonance to the  $|0\rangle$  to  $|1\rangle$  transition, giving rise to Rabi oscillation of the state population. Reading out the

qubit is accomplished by applying a short dc flux pulse to the qubit loop, during which only the excited qubit state may tunnel to the neighboring potential well. Since this tunneling event entails a flux quantum entering the qubit loop, reading out the qubit is concluded by a measurement of the flux threading the qubit loop by means of an inductively coupled DC-SQUID. Figure 3(a) shows a circuit schematic and 3(b) a micrograph of the tested sample. Here, a  $\pi$ -junction is connected in series to the phase qubit's tunnel junction. This circuit was fabricated in a standard Nb/Al-AlO<sub>x</sub>/Nb trilayer process, whereas the  $\pi$ -junction was integrated subsequently by performing the additional lithographic steps described above. Coherent qubit operation is demonstrated by the data reported in Fig. 4(a), showing Rabi oscillation of the excited qubit state population probability in dependence on the duration of a resonant microwave pulse. Each data set was taken using the indicated microwave power as delivered by the generator, giving rise to a change in the coherent oscillation frequency as expected for Rabi oscillation. The oscillations exhibit a decay time of about 4 ns, which is a typical value reachable in samples fabricated using similar fabrication processes [24]. To find out whether  $\pi$ -junction does introduce additional decoherence, a conventional phase qubit without a  $\pi$ -junction was fabricated on the same wafer. This qubit, however, required a constant phase bias of about  $\pi$  set by applying an external magnetic field. As shown in Fig. 4(b), this reference qubit shows a nearly identical decay time for Rabi oscillations, allowing us to conclude that at least on the observable time scale no extra decoherence is introduced by the SFS  $\pi$  phase shifter employed in this circuit.

We compared the measured decoherence time with the theoretical predictions [25]. We assume here an *overdamped* SFS  $\pi$ -junction having a normal resistance of  $R_{N,\pi} \approx 500 \mu\Omega$  and a critical current  $I_{C,\pi} \approx 50 \mu\text{A}$ . In our case, the qubit level splitting  $\Delta \gg 2eI_{C,\pi}R_{N,\pi}$ , where  $\Delta \approx h \cdot 13.5 \text{ GHz}$ ,  $h$  is the Plank's constant and  $e$  is the elementary charge. Here, the energy  $2eI_{C,\pi}R_{N,\pi} \approx h \cdot 12 \text{ MHz}$  is associated with characteristic Josephson frequency of our SFS  $\pi$ -junction. Simplifying the expression for the relaxation time [25] in this limit (see supplementary material), we can theoretically estimate the relaxation time  $\tau_{\text{relax}}$  as

$$\tau_{\text{relax}} \approx \frac{\Delta}{2I_C^2 R_{N,\pi}} \approx 2 \text{ ns}. \quad (1)$$

Here,  $I_C \approx 2 \mu\text{A}$  is the critical current of the small SIS qubit junction. The estimated value of the energy relaxation time is in good agreement with the measured decoherence time. We note, however, that the relaxation time (1) can be significantly enhanced by using SFS



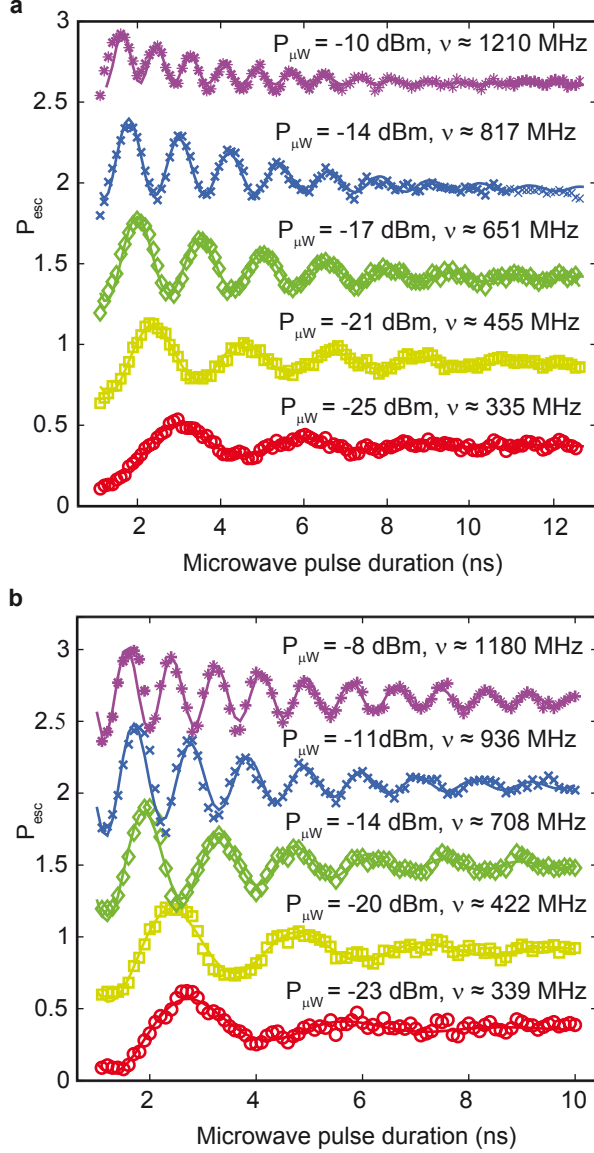


FIG. 4: Rabi oscillation of the occupation probability of the excited qubit state resulted from resonant microwave driving. **a**, Observed in the phase qubit with embedded  $\pi$ -junction, and **b**, A conventional phase qubit made on the same wafer as a reference.

junctions with a smaller resistance  $R_{N,\pi}$ .

In contrast to  $\pi$ -junctions based on high- $T_c$  superconductor junctions with  $d$ -wave pairing symmetry, SFS elements can have a sufficiently large critical current, so the desired  $\pi$  phase shift remains reliably fixed during circuit operation. In distinction from phase-shifting loops with frozen magnetic flux [20], the SFS circuits are much more compact and do not require

trapping a well-defined integer number flux quanta in their superconducting loops.

As an outlook, a significant reduction in the size of the demonstrated SFS  $\pi$ -phase shifters for digital circuits is readily possible. The visualization of the magnetic structure of our F layer material shows domain sizes smaller than 100 nm. Therefore, we believe that a reduction of the junction planar dimensions down to 300-500 nm is feasible. Furthermore, combining the high- $j_C$   $\pi$ -junction technology with in-situ grown tunnel barriers [26, 27] may open the way towards active inverter elements which are in great demand for superconducting electronics.

In summary, we demonstrated here the successful operation of three generic superconducting circuits with embedded  $\pi$ -junction phase shifters. For the studied  $\pi$ -biased phase qubit, we observed Rabi oscillations and compared their coherence time with that of conventional phase qubits fabricated by the same technology. We find no degradation of the coherence time induced by the presence of the  $\pi$ -junction. The demonstrated SFS  $\pi$ -junction phase shifter circuits are readily scalable and compatible with conventional niobium-based superconducting circuit technology.

- 
- [1] Bulaevskii, L. N., Kuzii, V. V. & Sobyanin, A. A. Superconducting system with weak coupling to the current in the ground state. *JETP Lett.* **25**, 290-294 (1977).
  - [2] Buzdin, A. I., Bulaevskij, L. N. & Panyukov, S. V. Critical-current oscillations as a function of the exchange field and thickness of the ferromagnetic metal (F) in an S-F-S Josephson junction. *JETP Lett.* **35**, 178-180 (1982).
  - [3] Van Harlingen, D. J. Phase-sensitive tests of the symmetry of the pairing state in the high-temperature superconductors—Evidence for  $d_{x^2-y^2}$  symmetry. *Rev. Mod. Phys.* **67**, 515-535 (1995).
  - [4] Testa, G. *et al.* Midgap state-based  $\pi$ -junctions for digital applications. *Appl. Phys. Lett.* **85**, 1202-1204 (2004).
  - [5] Hilgenkamp, H. *et al.* Ordering and manipulation of the magnetic moments in large-scale superconducting  $\pi$ -loop arrays. *Nature* **422**, 50-53 (2003).
  - [6] Baselmans, J. J. A., Morpurgo, A. F., van Wees, B. & Klapwijk, T. M. Reversing the direction of supercurrent in a controllable Josephson junction. *Nature* **397**, 43-45 (1999).

- [7] Ryazanov, V. V. *et al.* Coupling of two superconductors through a ferromagnet: evidence for a  $\pi$ -junction. *Phys. Rev. Lett.* **86**, 2427-2430 (2001).
- [8] Cleuziou, J.-P., Wernsdorfer, W., Bouchiat, V., Ondarcuhu, T. & Monthieux, M. Carbon nanotube superconducting quantum interference device. *Nature Nanotech.* **1**, 53-59 (2006).
- [9] Terzioglu, E. & Beasley, M. R. Complementary Josephson junction devices and circuits: a possible new approach to superconducting electronics. *IEEE Trans. Appl. Supercond.* **8**, 48-53 (1998).
- [10] Ustinov, A. V. & Kaplunenko, V. K. Rapid single-flux quantum logic using  $\pi$ -shifters. *J. Appl. Phys.* **94**, 5405-5407 (2003).
- [11] Ioffe, L. B., Geshkenbein, V. B., Feigelman, M. V., Fauchère, A. L. & Blatter, G. Environmentally decoupled sds-wave Josephson junctions for quantum computing. *Nature* **398**, 679-681 (1999).
- [12] Blatter, G., Geshkenbein, V. B. & Ioffe, L. B. Design aspects of superconducting-phase quantum bits. *Phys. Rev. B* **63**, 174511 (2001).
- [13] Buzdin, A. I. Proximity effects in superconductor-ferromagnet heterostructures. *Rev. Mod. Phys.* **77**, 935-976 (2005).
- [14] Frolov, S. M. *et al.* Imaging spontaneous currents in superconducting arrays of  $\pi$ -junctions. *Nature Phys.* **4**, 32-36 (2008).
- [15] Ryazanov, V. V., Oboznov, V. A., Veretennikov, A. V. & Rusanov, A. Y. Intrinsically frustrated superconducting array of superconductor-ferromagnet-superconductor  $\pi$  junctions. *Phys. Rev. B* **65**, 020501 (2001).
- [16] Frolov, S. M., Van Harlingen, D. J., Oboznov, V. A., Bolginov, V. V. & Ryazanov, V. V. Measurement of the current-phase relation of superconductor/ferromagnet/superconductor  $\pi$  Josephson junctions. *Phys. Rev. B* **70**, 144505 (2004).
- [17] Oboznov, V. A., Bolginov, V. V., Feofanov, A. K., Ryazanov, V. V. & Buzdin, A. I. Thickness dependence of the Josephson ground states of superconductor-ferromagnet-superconductor junctions. *Phys. Rev. Lett.* **96**, 197003 (2006).
- [18] Likharev, K. K. & Semenov, V. K. RSFQ logic/memory family: a new Josephson-junction technology for sub-terahertz-clock-frequency digital systems. *IEEE Trans. Appl. Supercond.* **1**, 3-28 (1991).
- [19] Ortlepp, T. *et al.* Flip-flopping fractional flux quanta. *Science* **312**, 1495-1497 (2006).

- [20] Majer, J. B., Butcher, J. R. & Mooij, J. E. Simple phase bias for superconducting circuits. *Appl. Phys. Lett.* **80**, 3638-3640 (2002).
- [21] Balashov, D. *et al.* Passive phase shifter for superconducting Josephson circuits. *IEEE Trans. Appl. Supercond.* **17**, 142-145 (2007).
- [22] Simmonds, R. W. *et al.* Decoherence in Josephson phase qubits from junction resonators. *Phys. Rev. Lett.* **93**, 077003 (2004).
- [23] Chiorescu, I., Nakamura, Y., Harmans, C. J. P. M. & Mooij, J. E. Coherent quantum dynamics of a superconducting flux qubit. *Science* **299**, 1869-1871 (2003).
- [24] Lisenfeld, J., Lukashenko, A., Ansmann, M., Martinis, J. M. & Ustinov, A. V. Temperature dependence of coherent oscillations in Josephson phase qubits. *Phys. Rev. Lett.* **99**, 170504 (2007).
- [25] Kato, T., Golubov, A. A. & Nakamura, Y. Decoherence in a superconducting flux qubit with a  $\pi$ -junction. *Phys. Rev. B* **76**, 172502 (2007).
- [26] Weides, M. *et al.* 0- $\pi$  Josephson Tunnel Junctions with Ferromagnetic Barrier. *Phys. Rev. Lett.* **97**, 247001 (2006).
- [27] Bannykh, A. A. *et al.* Josephson tunnel junctions with a strong ferromagnetic interlayer. *Phys. Rev. B* **79**, 054501 (2009).
- [28] Burmistrov, E. V. *et al.* A planar picoamperemeter based on a superconducting quantum interferometer. *J. Commun. Technol. Electr.* **51**, 1319-1324 (2006).

## ACKNOWLEDGEMENTS

This work was supported by the EU projects EuroSQIP and MIDAS. We acknowledge support by the Deutsche Forschungsgemeinschaft (DFG), the joint grant of DFG and Russian Foundation of Basic Research, the Russian Federal Agency of Science and Innovations, and the State of Baden-Württemberg through the DFG Center for Functional Nanostructures (CFN).

## COMPETING INTERESTS

The authors declare that they have no competing financial interests.

## CORRESPONDENCE

Correspondence and requests for materials should be addressed to A.V. Ustinov (email: [ustinov@physik.uni-karlsruhe.de](mailto:ustinov@physik.uni-karlsruhe.de)).

## SUPPLEMENTARY MATERIALS

### Sample fabrication

For fabrication of SFS  $\pi$ -junctions, the bottom Nb-electrode with thickness of 110 nm was fabricated by dc-magnetron sputtering followed by a lift-off process. The deposition of the copper-nickel layer (F layer) was carried out by rf sputtering after ion cleaning of the niobium surface. Afterwards, the insulating layer having a  $10 \times 10 \mu\text{m}^2$  window which determines the junction area was prepared by the lift-off process. We used a 150 nm thick SiO film as insulator, which was thermally evaporated. The fabrication procedure was completed by Ar plasma cleaning and dc-magnetron sputtering of the upper niobium electrode of 240 nm thickness.

Details on the fabrication technique for tunnel Nb/Al/AlO<sub>x</sub>/Nb junctions employed in this circuit are presented in Ref. [28]. In brief, a three-layer Nb/Al/AlO<sub>x</sub>/Nb structure is deposited by magnetron sputtering. The layers have thicknesses of 180, 7, and 80 nm, respectively. Aluminum is oxidized in pure oxygen to form a tunnel barrier having a critical current density of about 200 A/cm<sup>2</sup>. The junction area, here  $10 \mu\text{m}^2$ , is defined by reactive ion etching and subsequent SiO<sub>2</sub> deposition. Resistive shunts in parallel to the tunnel junctions are formed by a molybdenum layer with a specific resistance of 2  $\Omega$  per square.

### Estimates of decoherence in $\pi$ -junctions

In the paper by Kato, Golubov and Nakamura [25], the following expressions for the effective noise spectrum  $J_{\text{eff}}$  and relaxation time  $\tau_{\text{relax}}$  were obtained:

$$J_{\text{eff}}(\omega) = \frac{8E_J^2 E_{C,\pi}}{\hbar^3} \left[ \frac{\gamma\omega}{\gamma^2\omega^2 + (\omega^2 - \omega_0^2)^2} \right], \quad (2)$$

where  $\gamma = \frac{1}{R_\pi C_\pi}$ ,  $\omega_0 = \frac{\sqrt{8E_{J,\pi}E_{C,\pi}}}{\hbar}$ ,  $E_{C,\pi} = \frac{e^2}{2C_\pi}$  and

$$\tau_{\text{relax}}^{-1} = 2J_{\text{eff}}(\Delta/\hbar) \coth\left(\frac{\Delta}{2k_B T}\right), \quad (3)$$

where  $\Delta$  is the qubit level splitting. These equations were derived using an RSJ model under an assumption  $E_{J,\pi} \gg E_J \gg E_C$ , which means the  $\pi$ -junction remains in the superconducting state and we are working in the regime of a well defined phase.

Assuming that  $\omega \ll \omega_0$ , we can write

$$J_{\text{eff}}(\omega) \approx \frac{8E_J^2 E_{C,\pi}}{\hbar^3} \left[ \frac{\gamma\omega}{\gamma^2\omega^2 + \omega_0^4} \right] = \quad (4)$$

$$= \frac{8E_J^2 E_{C,\pi}}{\hbar^3} \left[ \frac{\gamma\omega}{\gamma^2\omega^2 + 64 \frac{E_{J,\pi}^2 E_{C,\pi}^2}{\hbar^4}} \right] = \quad (5)$$

$$= \frac{4E_J^2 \frac{e^2}{R_{N,\pi} C_\pi^2} \omega}{\frac{\hbar^3}{R_{N,\pi}^2 C_\pi^2} \left[ \omega^2 + 16 \frac{E_{J,\pi}^2}{\hbar^4} e^4 R_{N,\pi}^2 \right]}. \quad (6)$$

Now we can exclude  $C_\pi$ ,

$$J_{\text{eff}}(\omega) \approx \frac{4E_J^2 e^2 R_{N,\pi} \omega}{\hbar^3 \left[ \omega^2 + 16 \frac{E_{J,\pi}^2}{\hbar^4} e^4 R_{N,\pi}^2 \right]}. \quad (7)$$

Since  $E_J = \frac{I_C \Phi_0}{2\pi} = \frac{I_C \hbar}{2e}$ , it allows us to further simplify the latter expression:

$$J_{\text{eff}}(\omega) \approx \frac{4 \frac{I_C^2 \hbar^2}{4e^2} e^2 R_{N,\pi} \omega}{\hbar^3 \left[ \omega^2 + 16 \frac{I_{C,\pi}^2 \hbar^2}{4e^2} \frac{e^4}{\hbar^4} R_{N,\pi}^2 \right]} = \quad (8)$$

$$= \frac{I_C^2 R_{N,\pi} \hbar \omega}{\hbar^2 \omega^2 + 4e^2 I_{C,\pi}^2 R_{N,\pi}^2}. \quad (9)$$

The relaxation time can be calculated as

$$\tau_{\text{relax}} = \left[ 2J_{\text{eff}}(\Delta/\hbar) \coth\left(\frac{\Delta}{2k_B T}\right) \right]^{-1} \approx \quad (10)$$

$$\approx \left[ 2 \left( \frac{I_C^2 R_{N,\pi} \hbar \frac{\Delta}{\hbar}}{\hbar^2 \left( \frac{\Delta}{\hbar} \right)^2 + 4e^2 I_{C,\pi}^2 R_{N,\pi}^2} \right) \coth\left(\frac{\Delta}{2k_B T}\right) \right]^{-1} = \quad (11)$$

$$= \left( \frac{\Delta^2 + 4e^2 I_{C,\pi}^2 R_{N,\pi}^2}{2I_C^2 R_{N,\pi} \Delta} \right) \tanh\left(\frac{\Delta}{2k_B T}\right). \quad (12)$$

If the qubit level splitting  $\Delta \gg 2eI_{C,\pi}R_{N,\pi}$  we can neglect the second term in the numerator:

$$\tau_{\text{relax}} \approx \left( \frac{\Delta}{2I_C^2 R_{N,\pi}} \right) \tanh\left(\frac{\Delta}{2k_B T}\right) \approx 2 \text{ ns}. \quad (13)$$

In our case  $\Delta \approx h \cdot 13.5 \text{ GHz}$ ,  $I_C \approx 2 \mu\text{A}$ ,  $R_{N,\pi} \approx 500 \mu\Omega$ . The temperature  $T$  was about 50 mK, thus  $\tanh\left(\frac{\Delta}{2k_B T}\right) \approx 1$ .